Radiology

ORIGINAL RESEARCH • THORACIC IMAGING

Chest CT Patterns from Diagnosis to 1 Year of Follow-up in Patients with COVID-19

*Feng Pan, MD** • *Lian Yang, MD** • *Bo Liang, MD* • *Tianhe Ye, MD* • *Lingli Li, MD* • *Lin Li, MD* • *Dehan Liu, MD* • *Jiazheng Wang, PhD* • *Richard L. Hesketh, MD, PhD* • *Chuansheng Zheng, MD, PhD*

From the Department of Radiology, Union Hospital, Tongji Medical College, Huazhong University of Science and Technology, Jiefang Ave 1277, Wuhan 430022, China (F.P., L.Y., B.L., T.Y., Lingli Li, Lin Li, D.L., C.Z.); Hubei Province Key Laboratory of Molecular Imaging, Wuhan, China (F.P., L.Y., B.L., T.Y., Lingli Li, Lin Li, D.L., C.Z.); MSC Clinical and Technical Solutions, Philips Healthcare, Beijing, China (J.W.); and Department of Radiology, University College London Hospital, London, England (R.L.H.). Received May 10, 2021; revision requested June 14; revision received September 5; accepted September 9. **Address correspondence to** C.Z. (e-mail: *hqzcsxh@sina.com*).

Supported by the Rapid Response Key Project of COVID-19 at Huazhong University of Science and Technology (grant no. 2020kfyXGYJ021) and the Key Special Project of the Ministry of Science and Technology, China (grant no. 2020YFC0845700).

* F.P. and L.Y. contributed equally to this work.

Conflicts of interest are listed at the end of this article.

See also the editorial by Lee and Wi et al in this issue.

Radiology 2022; 302:709–719 • https://doi.org/10.1148/radiol.211199 • Content codes: CH CT

Background: The chest CT manifestations of COVID-19 from hospitalization to convalescence after 1 year are unknown.

Purpose: To assess chest CT manifestations of COVID-19 up to 1 year after symptom onset.

Materials and Methods: Patients were enrolled if they were admitted to the hospital because of COVID-19 and underwent CT during hospitalization at two isolation centers between January 27, 2020, and March 31, 2020. In a prospective study, three serial chest CT scans were obtained at approximately 3, 7, and 12 months after symptom onset and were longitudinally analyzed. The total CT score of pulmonary lobe involvement, ranging from 0 to 25, was assessed (score of 1–5 for each lobe). Univariable and multivariable logistic regression analyses were performed to explore independent risk factors for residual CT abnormalities after 1 year.

Results: A total of 209 study participants (mean age, 49 years ± 13 [standard deviation]; 116 women) were evaluated. CT abnormalities had resolved in 61% of participants (128 of 209) at 3 months and in 75% of participants (156 of 209) at 12 months. Among participants with chest CT abnormalities that had not resolved, there were residual linear opacities in 25 of the 209 participants (12%) and multifocal reticular or cystic lesions in 28 of the 209 participants (13%). Age 50 years or older, lymphopenia, and severe or aggravation of acute respiratory distress syndrome were independent risk factors for residual CT abnormalities at 1 year (odds ratios = 15.9, 18.9, and 43.9, respectively; $P < .001$ for each comparison). In 53 participants with residual CT abnormalities at 12 months, reticular lesions (41 of 53 participants [77%]) and bronchial dilation (39 of 53 participants [74%]) were observed at discharge and were persistent in 28 (53%) and 24 (45%) of the 53 participants, respectively.

Conclusion: One year after COVID-19 diagnosis, chest CT scans showed abnormal findings in 53 of the 209 study participants (25%), with 28 of the 209 participants (13%) showing subpleural reticular or cystic lesions. Older participants with severe COVID-19 or acute respiratory distress syndrome were more likely to develop lung sequelae that persisted at 1 year.

Online supplemental material is available for this article.

Since the global outbreak of the COVID-19 pandemic, more than 100 million people have been infected, resulting in more than three million deaths globally (1). Several of the β coronaviruses have similar clinical course and laboratory, radiologic, and pathologic features. These coronaviruses include severe acute respiratory syndrome (SARS), Middle East respiratory syndrome, and COVID-19 (2–5). However, SARS coronavirus 2 has proven more contagious than other coronaviruses, resulting in a far higher number of cases and a global pandemic (1,6).

Previous chest CT observations of COVID-19 have demonstrated a typical radiologic course from initial bilateral and subpleural ground-glass opacities (GGOs) to a more extensive consolidation, with slow but gradual absorption of the lung lesions in survivors (7–11). However, residual pulmonary lesions, such as GGOs and parenchymal bands, have been observed in more than 90% of patients at hospital discharge (7,9). Because coronavirus infection can result in diffuse alveolar exudation and can lead to fatal acute respiratory distress syndrome (ARDS), postinfection sequelae, such as lung fibrosis, are a concern (12,13). Focal lung fibrosis seen at chest CT has been observed in patients who have recovered from SARS, even after a 7-year follow-up (14,15). Although lung lesions mostly resolve in COVID-19 with mild to moderate severities, an autopsy study has confirmed lung organization and fibrosis in patients with fatal COVID-19, raising the possibility of permanent lung fibrosis sequelae in survivors with severe infection (7,16). In some patients with COVID-19, fibrotic sequelae, including traction bronchiectasis, parenchymal bands, and "honeycombing," have been observed in more than one-third of participants with severe COVID-19 at 6 months after symptom onset (7,17). However, it is unknown whether COVID-19 survivors develop lung fibrosis after a long follow-up period and whether risk factors at presentation are predictive of long-term loss of function. If so, chest CT could potentially

Abbreviations

ARDS = acute respiratory distress syndrome, GGO = ground-glass opacity, SARS = severe acute respiratory syndrome

Summary

One year after COVID-19 diagnosis, chest CT scans showed persistent abnormalities in 53 of 209 adult study participants (25%).

Key Results

- A total of 209 individuals who had been hospitalized with COVID-19 underwent serial chest CT examinations at approximately 3, 7, and 12 months.
- CT scans obtained at 1-year follow-up showed one of three patterns—complete resolution (156 of 209 participants [75%]), residual linear opacities (25 of 209 participants [12%]), or multifocal reticular or cystic lesions (28 of 209 participants [13%]).
- Independent risk factors for long-term chest CT changes at 1 year included age 50 years or older, lymphopenia, and severe or aggravation of acute respiratory distress syndrome (odds ratio = 15.9, 18.9, and 43.9, respectively; $P < .001$ for each comparison).

help identify patients who might benefit from early antifibrotic therapy (18). The purpose of our study was to evaluate serial chest CT examinations for the 1-year temporal evolution of radiologic findings after COVID-19 infection.

Materials and Methods

This study was approved by the Ethics Committees of Union Hospital of Tongji Medical College at Huazhong University of Science and Technology (serial no. 2020–0026) and followed the 1964 Helsinki Declaration and its later amendments. All study participants provided informed consent.

Study Sample

We prospectively evaluated participants with COVID-19 consecutively discharged from two isolation centers (ie, Western Campus and Zhuankou Fangcang Shelter Hospitals, affiliated with Union Hospital of Tongji Medical College at Huazhong University of Science and Technology) between January 27, 2020, and March 31, 2020. This cohort included participants reported in a previous study that involved only data at admission and discharge for the longitudinal analysis in our study (7). The criteria for diagnosis, therapy, and discharge followed the nationally standardized protocols (19). Patients with a respiratory rate greater than 30 breaths per minute or an oxygen saturation of 93% or less while breathing room air were classified as having severe COVID-19, whereas ARDS was diagnosed when the ratio of arterial partial pressure of oxygen to fraction of inspired oxygen was 300 mm Hg or less (19–21). The inclusion criteria were as follows: *(a)* age 18 years or older; *(b)* no medical history of pulmonary, autoimmune, or malignant disease; *(c)* COVID-19 survivors who underwent hospitalized treatment; *(d)* chest CT performed at admission and discharge; *(e)* chest CT at discharge showing residual lung lesions related to COVID-19; and *(f)* voluntary, written informed consent for chest CT follow-up. We excluded participants who dropped out of the study, had a subsequent positive result after a COVID-19 nucleic acid test, or acquired an additional lung infection after discharge.

Chest CT Protocol

Unenhanced chest CT examinations were performed using the same commercial CT scanner (Ingenuity Core 128, Philips Medical Systems). Images were obtained during breath holding at full inspiration. The fixed tube voltage was set to 120 kVp with adaptive current modulation, resulting in a mean volume CT dose index of 7.1 mGy ± 2.2 (standard deviation) (range, 3.1–12.2 mGy) and a dose-length product of 286.0 mGy · cm ± 97.2 (range, 99.2–506.3 mGy · cm). Other acquisition parameters were as follows: pitch, 0.999; collimation, 64 × 0.625 mm; gantry rotation time, 0.75 second; and DoseRight (Philips) index, 18. From the raw data, axial CT scans were reconstructed with a matrix size of

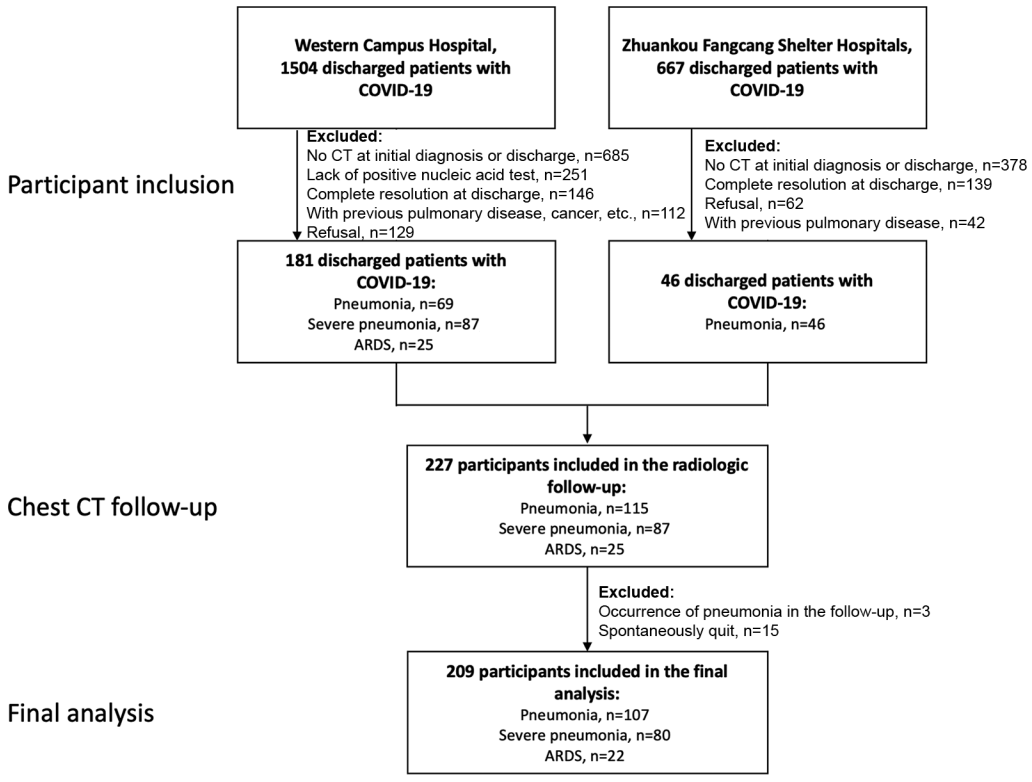

Figure 1: Flowchart of participant inclusion. ARDS = acute respiratory distress syndrome.

Table 1: Basic Characteristics of Study Sample

Characteristic	Value
Age (y)*	49 ± 13 (20–82)
Sex	
Men	93/209 (45)
Women	116/209 (56)
Comorbidity	41/209 (20)
Hypertension	28/41 (68)
Type 2 diabetes mellitus	13/41 (32)
Coronary heart disease	11/41 (27)
Smoking history	4/209 (1.9)
Initial symptom	
Fever	177/209 (85)
Cough	91/209 (44)
Chest distress	25/209 (12)
Fatigue	27/209 (13)
Myalgia	15/209 (7)
Headache	5/209 (2.4)
Diarrhea	2/209 (1.0)
Time between admission and initial symptom onset (d)*	6.9 ± 4.4 (1.0–18.0)
COVID-19 severity	
Pneumonia	107/209 (51)
Severe pneumonia	80/209 (38)
Acute respiratory distress syndrome	22/209 (11)
Length of hospital stay (d)*	24.8 ± 13.3 (5.0–80.0)
Laboratory results at admission†	
White blood cell count ($\times 10^9$/L)	6.07 ± 2.67 (2.25–21.00) [3.50–9.50]
Lymphocyte count ($\times 10^9$/L)	1.13 ± 0.42 (0.26–3.10) [1.10–3.20]
Hemoglobin level (g/L)	127 ± 16 (77–169) [115–150]
Hematocrit level (%)	38.6 ± 8.9 (23.4–134.0) [35.0–45.0]
Platelet count ($\times 10^9$/L)	219 ± 80 (45–498) [125–350]
Aspartate transaminase level (U/L)	32 ± 18 (11–108) [5–35]
Alanine aminotransferase level (U/L)	41 ± 34 (9–234) [8–40]
Lactate dehydrogenase level (U/L)	250 ± 168 (98–1633) [109–245]
Total bilirubin level (μmol/L)	12.1 ± 7.8 (2.8–69.7) [3.0–20]
Albumin level (g/L)	33.9 ± 6.6 (20.1–49.6) [33–55]
Blood urea nitrogen level (mmol/L)	4.45 ± 1.63 (1.49–9.51) [2.9–8.2]
Serum creatinine level (μmol/L)	65.9 ± 17.5 (39.4–170.8) [41–81]
Time between chest CT examinations and symptom onset (d)*	
At admission	6.3 ± 4.5 (0.0–20.0)
At discharge	28.3 ± 13.8 (6.0–76.0)

Note.—Except where indicated, data are numbers of participants (n = 209), with percentages in parentheses.

* Numbers are means ± standard deviations, with ranges in parentheses.

† Numbers are means ± standard deviations, with ranges in parentheses and normal reference ranges in brackets.

512 × 512 (thickness of 1.5 mm and interval of 1.5 mm) using iterative reconstruction (iDose level 5, Philips Healthcare).

Serial Chest CT Assessments

Chest CT data at admission and discharge were retrospectively collected from the institutional picture archiving and communication system (version 11.3.5.8902, Vue PACS; Carestream Health). In addition, three serial chest CT examinations were performed at 3, 7, and 12 months since initial symptom onset. Visual assessments were independently performed by three senior radiologists (B.L., L.Y., and C.Z., with 26, 23, and 27 years of clinical experience in thoracic radiology, respectively). Afterward, any disagreement was resolved by discussion and consensus. Three radiologists were blinded to the clinical progress of all participants. Abnormalities were described using the standard terms defined in the Fleischner Society glossary and peer-reviewed literature (Fig E1 [online]) (7,8,11,17,22–24). Complete resolution was defined as the disappearance of any COVID-19–related lung abnormalities at chest CT (7). The distribution of lung lesions was categorized as a subpleural, diffuse, or random distribution (8). Following the methods in previous studies of COVID-19, we used the same semiquantitative CT scoring system to estimate the involvement of the lung lesions in each lobe from 0 to 5 points (ie, 0, no lesion; 1, <5%; 2, 5%–25%; 3, 26%–49%; 4, 50%–75%; 5, >75%) (8,17,25). The sum of the CT score in each lobe was calculated as the total CT score, ranging from 0 to 25. At 12 months after symptom onset, participants with or without residual CT abnormalities were compared.

Statistical Analysis

All statistical analyses were performed using SPSS statistics software (version 26, IBM). Quantitative and counting data were presented as means ± standard deviations, with ranges and the percentages of the total, respectively. Mann-Whitney tests were performed to estimate continuous variables between different groups according to the nonnormal distribution assessed with the Shapiro-Wilk tests. We performed χ^2 tests to evaluate categoric variables between different groups. The Fisher exact test was performed instead of a χ^2 test if the expected count was less than five. Univariable and multivariable logistic regression analyses (ie, forward conditional method) were used to investigate the independent risk factors for chronic CT changes after 1 year, and odds ratios with 95% CIs were calculated. Linear mixed models of repeated measures were established to estimate the fixed effects of the time and participant grouping on the number of involved lung lobes and total CT score

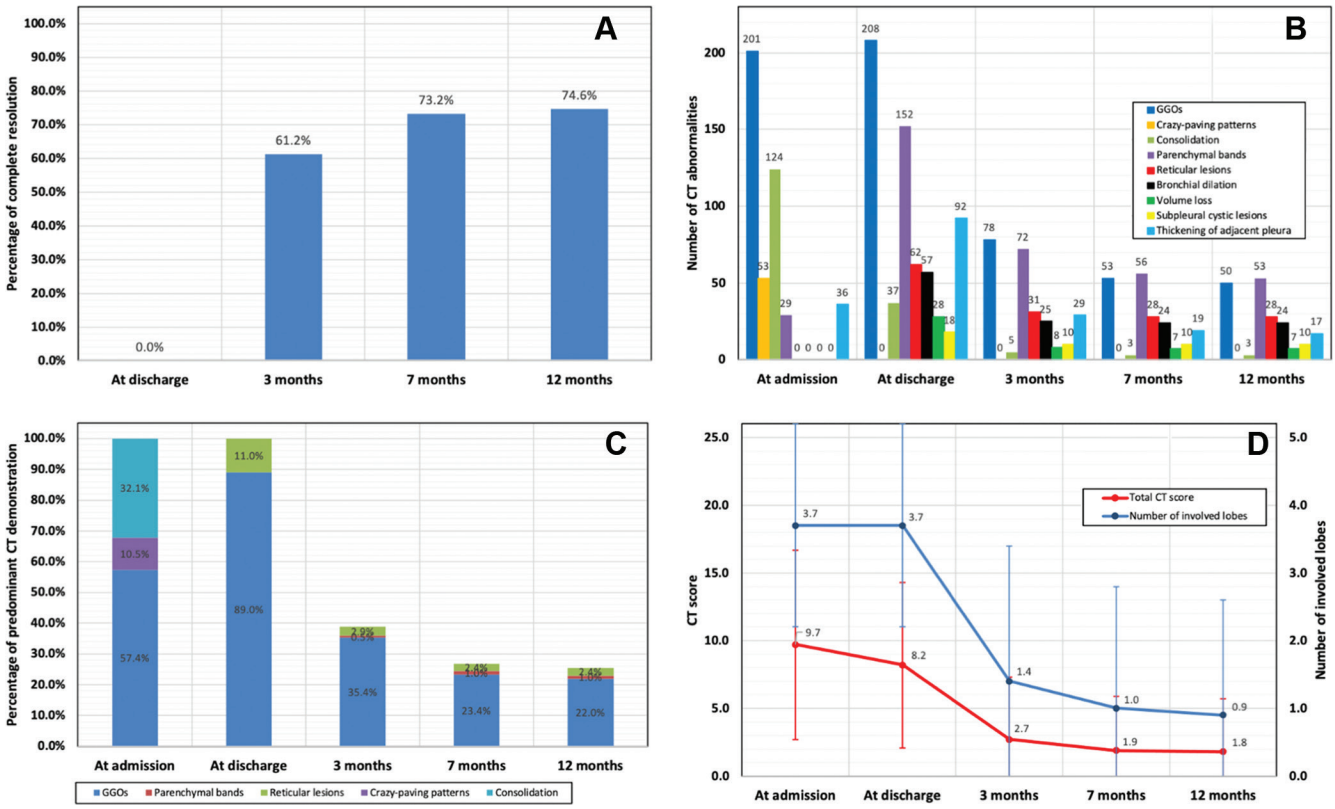

Figure 2: Graphs show dynamic CT changes over time. **(A)** Bar graph shows complete radiologic resolution. **(B)** Bar graph shows observable lung abnormalities. **(C)** Bar graph shows predominant CT abnormalities. **(D)** Graph shows mean total CT score with standard deviation bar and number of involved lobes. Linear mixed model of repeated measures was established to estimate fixed effects of time on total CT score (**D**) and number of involved lung lobes (**D**) using type III tests, and *P* values of multiple comparisons were obtained with Bonferroni adjustments. Significant decreases of mean total CT score (**D**) and number of involved lung lobes (**D**) were seen at 3 months ($P < .001$ for both comparisons). GGO = ground-glass opacity.

using type III tests. Further intertime point comparisons were performed using Bonferroni adjustments. Statistical significance was defined as two-tailed $P < .001$.

Results

Characteristics of Study Sample

A total of 2171 patients discharged from the hospital were screened for our study. Of these, 209 participants were included in the final analysis, 1063 patients were excluded owing to the lack of chest CT at admission, and 285 patients were excluded because of complete resolution of CT abnormalities at discharge (Fig 1). During follow-up, 15 patients were excluded because of study dropout, and three were excluded because of secondary lung infection (Fig 1). The mean age of participants was 49 years ± 13 (range, 20–82 years), with a 1:1.25 male-to-female ratio. Twenty percent of participants (41 of 209) had comorbidities, including hypertension, type 2 diabetes mellitus, and coronary heart disease. Four of 209 participants (2%) had a history of smoking. The mean interval between symptom onset and admission was 6.9 days ± 4.4 (range, 1.0–18.0 days). Pneumonia, severe pneumonia, and ARDS were diagnosed in 107 (51%), 80 (38%), and 22 (11%) participants, respectively. All participants who developed ARDS underwent mechanical ventilation in an intensive care unit. The mean hospitalized period was 24.8 days ± 13.3 (range, 5.0–80.0 days). The chest CT examinations at admission and discharge were performed at 6.3 days ± 4.5 and 28.3 days ± 13.8 after symptom onset, respectively. The detailed information is summarized in Table 1.

Visual CT Assessments

The complete resolution rate gradually increased over time from 61% (128 of 209 participants) at 3 months to 75% (156 of 209 participants) at 12 months after symptom onset (Fig 2A and Table E1 [online]). At admission, GGOs (201 of 209 participants [96%]), consolidation (124 of 209 participants [59%]), and "crazy paving" pattern (53 of 209 participants [25%]) were the most common findings (Fig 2B and Table E1 [online]). Thereafter, consolidation and crazy paving gradually improved over time, whereas other pulmonary abnormalities, including GGOs, parenchymal bands, reticular lesions, bronchial dilation, and volume loss, tended to increase after admission but started to resolve after discharge (Fig 2B and Table E1 [online]). However, at 3 months after symptom onset, CT abnormalities had stabilized except for GGOs and parenchymal bands, which gradually resorbed (Fig 2B and Table E1 [online]). Nevertheless, GGOs were the predominant radiologic pattern throughout (Fig 2C and Table E1 [online]). The mean total CT score and the number of involved lung lobes gradually decreased from admission (9.7 ± 7.0 and 3.7 ± 1.5, respectively) to 12 months (1.8 ± 3.9 and 0.9 ± 1.7, respectively) after symptom onset ($P < .001$ for both) (Fig 2D, Table E1

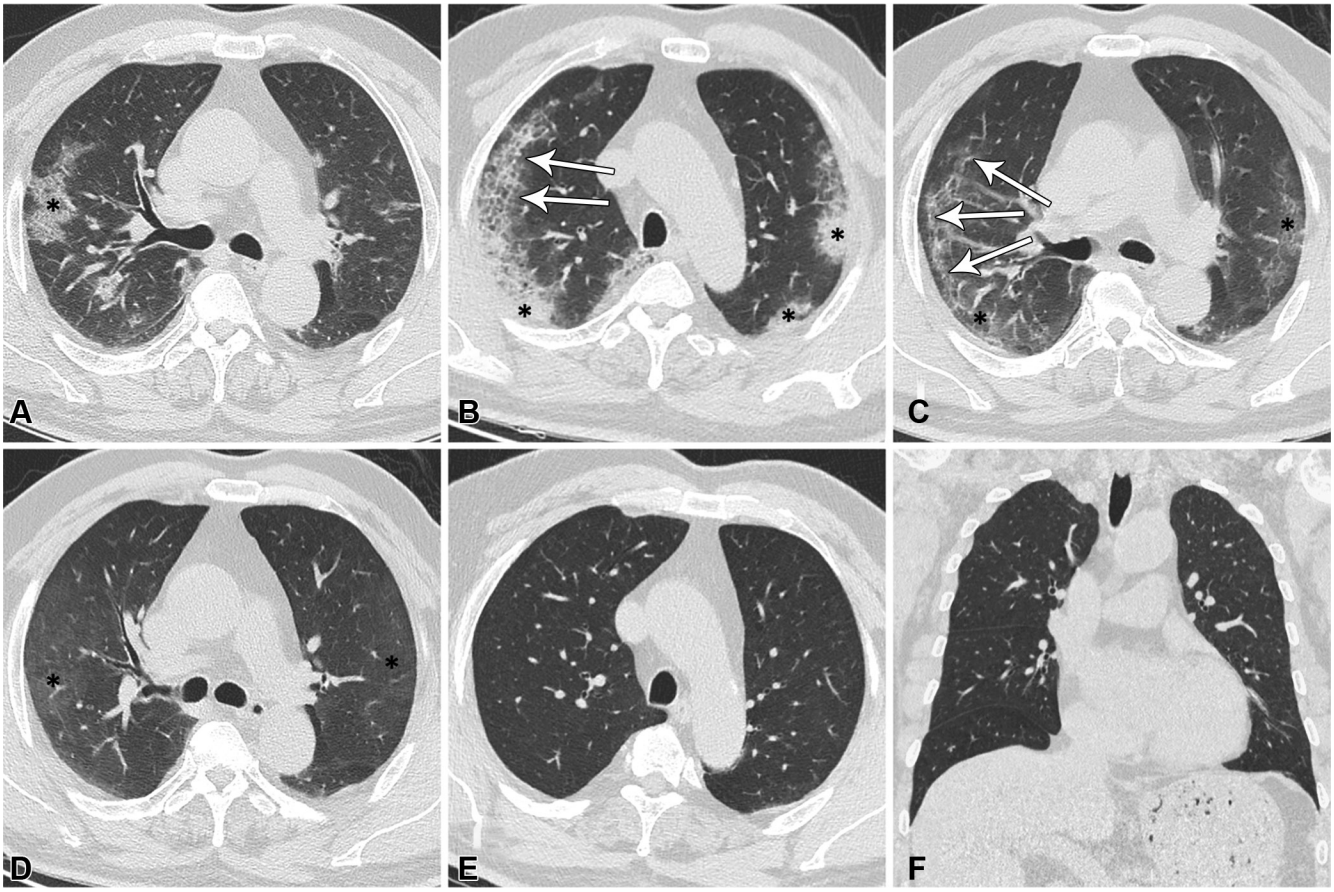

Figure 3: CT scans in 60-year-old man diagnosed with COVID-19 pneumonia show typical CT findings over time for participants with complete resolution. **(A)** Eleven days after symptom onset, CT scan shows bilateral, predominantly subpleural, ground-glass opacity (GGO) with foci of consolidation and "crazy paving" appearance (*). **(B)** Twenty-four days after symptom onset, enlarged areas of bilateral subpleural consolidation (*) and "crazy paving" appearance (arrows) are shown. **(C)** Thirty-six days after symptom onset, CT scan at discharge shows apparent absorption of consolidation, leaving residual and extensive GGOs (*) with blurry linear opacities (arrows) parallel to pleura. **(D)** Three months after symptom onset, CT scan shows continued resolution with residual GGOs (*) bilaterally. **(E)** Seven months after symptom onset, CT scan shows complete resolution of abnormalities. **(F)** Twelve months after symptom onset, CT scan shows no other delayed sequelae. All images have same window level of −600 HU and window width of 1600 HU.

[online]). After 3 months, the decrease in mean total CT score and mean number of involved lung lobes became nonsignificant ($P \geq 0.33$ and $P \geq .06$, respectively) (Fig 2D).

Comparisons between Participants with or without Complete Resolution at 12 Months

Participants were divided into two groups based on the CT abnormalities at 12 months after symptom onset—participants with complete resolution (156 of 209 participants [75%]) (Fig 3) and participants with residual CT abnormalities (53 of 209 participants [25%]) (Figs 4, 5). In participants with complete resolution, no recurrent pulmonary abnormalities were observed at further follow-up after complete resolution was initially achieved (Fig 3). Age, previous comorbidities, COVID-19 severities, time between admission and symptom onset, hospitalized period, lymphocyte count, lactate dehydrogenase level, albumin level, number of involved lobes, and total CT score at admission all demonstrated differences between the two groups ($P \leq .001$ for each comparison) (Tables 2, 3). Age 50 years or older, lymphopenia, and severe or aggravation of ARDS were independent risk factors for residual CT abnormalities at 1 year (odds ratio = 15.9, 18.9, and 43.9, respectively; $P < .001$ for each comparison) (Table 4).

Diffuse consolidation was more common at chest CT at admission and discharge in participants with residual CT abnormalities than in those with complete resolution (Table 3). At discharge, complicated CT abnormalities, including reticular lesions, bronchial dilation, and volume loss, were more commonly observed in participants with residual CT abnormalities than in participants with complete resolution, whereas predominant GGOs were common to both groups (Table 3). Over time, the total CT score and number of involved lung lobes gradually decreased, with statistically significant improvements at 3 months (Fig 6) but were higher in participants with residual CT abnormalities than participants with complete resolution (Table E2 [online]). Noticeably in participants with complete resolution, reticular lesions (21 of 156 participants [14%]) and bronchial dilation (18 of 156 participants [12%]) were observed at discharge but had almost completely resorbed at 3 months (Fig 6 and Fig E2 [online]). In participants with residual

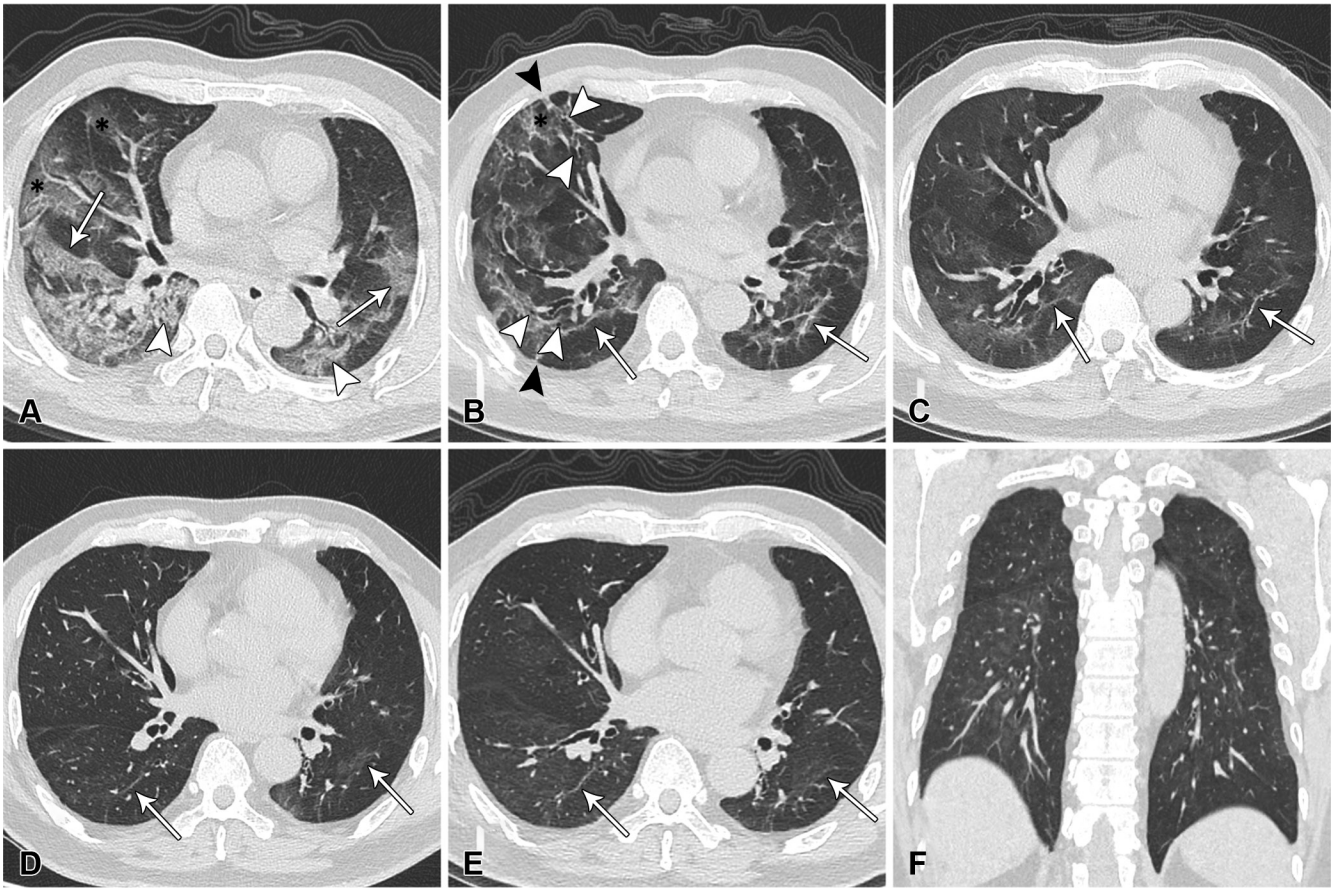

Figure 4: CT scans in 64-year-old man, who progressed to acute respiratory distress syndrome caused by COVID-19, show typical findings over time for participants with residual linear opacities. **(A)** Eight days after symptom onset, CT scan shows bilaterally diffuse mixed lesions, including ground-glass opacities (GGOs) (*), "crazy paving" appearance (arrows), and consolidation (arrowheads). **(B)** Fifty-two days after symptom onset, CT scan at discharge shows extensive GGOs and residual linear opacities (arrows), with focal volume loss indicated by displacement of major fissures, adjacent thickening of pleura, bronchial dilation (white arrowheads), parenchymal bands (black arrowheads), and reticular lesions (*). **(C)** Three months after symptom onset, CT scan shows continued resolution, with only residual GGOs and residual linear opacities (arrows) in bilateral lungs. **(D)** Seven months after symptom onset, bilateral GGOs and residual linear opacities (arrows) continue to be partially absorbed. Twelve months after symptom onset, **(E)** CT scan shows stable residual GGOs and residual linear opacities (arrows) compared with **(F)** previous CT scan, which shows them predominantly distributed in dorsal regions. All images have same window level of −600 HU and window width of 1600 HU.

CT abnormalities, reticular lesions (41 of 53 participants [77%]) and bronchial dilation (39 of 53 participants [74%]) observed at discharge were incompletely resorbed and persisted in 53% (28 of 53) and 45% (24 of 53) of participants at 12 months, respectively (Figs 4–6; Table E2 [online]).

Different Residual Abnormalities at 12 Months

On the basis of the different residual CT abnormalities at 12 months, participants could be further divided into two subgroups (Table E3 [online]): participants with residual linear opacities (25 of 53 participants [47%]) and those with multifocal reticular or cystic lesions (28 of 53 participants [53%]). Participants with residual linear opacities demonstrated gradual resolution of pulmonary lesions since discharge, leaving residual parenchymal bands or thin linear opacities (Fig 4; Figs E3, E4 [online]; Table E4 [online]). In contrast, participants with multifocal reticular or cystic lesions presented persistent subpleural reticular or cystic lesions at follow-up (Fig 5; Figs E4, E5, and Table E4 [online]). At 12 months, the total CT score was 3.9 ± 2.6 versus 10.1 ± 4.3, and the number of involved lung lobes was 2.6 ± 1.0 versus 4.5 ± 1.2 in participants with residual linear opacities and multifocal reticular or cystic lesions, respectively ($P < .001$ for both comparisons) (Tables E3, E4 [online]). However, the improvements in total CT scores in both subgroups were observed at 3 months after symptom onset ($P < .001$) (Fig E4 [online]).

Discussion

This study analyzed the chest CT patterns of 209 participants with COVID-19 over 1 year after symptom onset. On the basis of the CT findings at 12 months, participants could be categorized into three groups—complete resolution (156 of 209 [75%]), residual linear opacities (25 of 209 [12%]), and multifocal reticular or cystic lesions (28 of 209 [13%]). Complete resolution mainly occurred in the first 3 months after symptom onset (128 of 209 [61%]). After 3 months, residual lesions became increasingly persistent, highlighted by the insignificant decrease in total CT score from 2.7 ± 4.6 to 1.8 ± 3.9 at 3 and 12 months, respectively ($P = .33$). Compared with par-

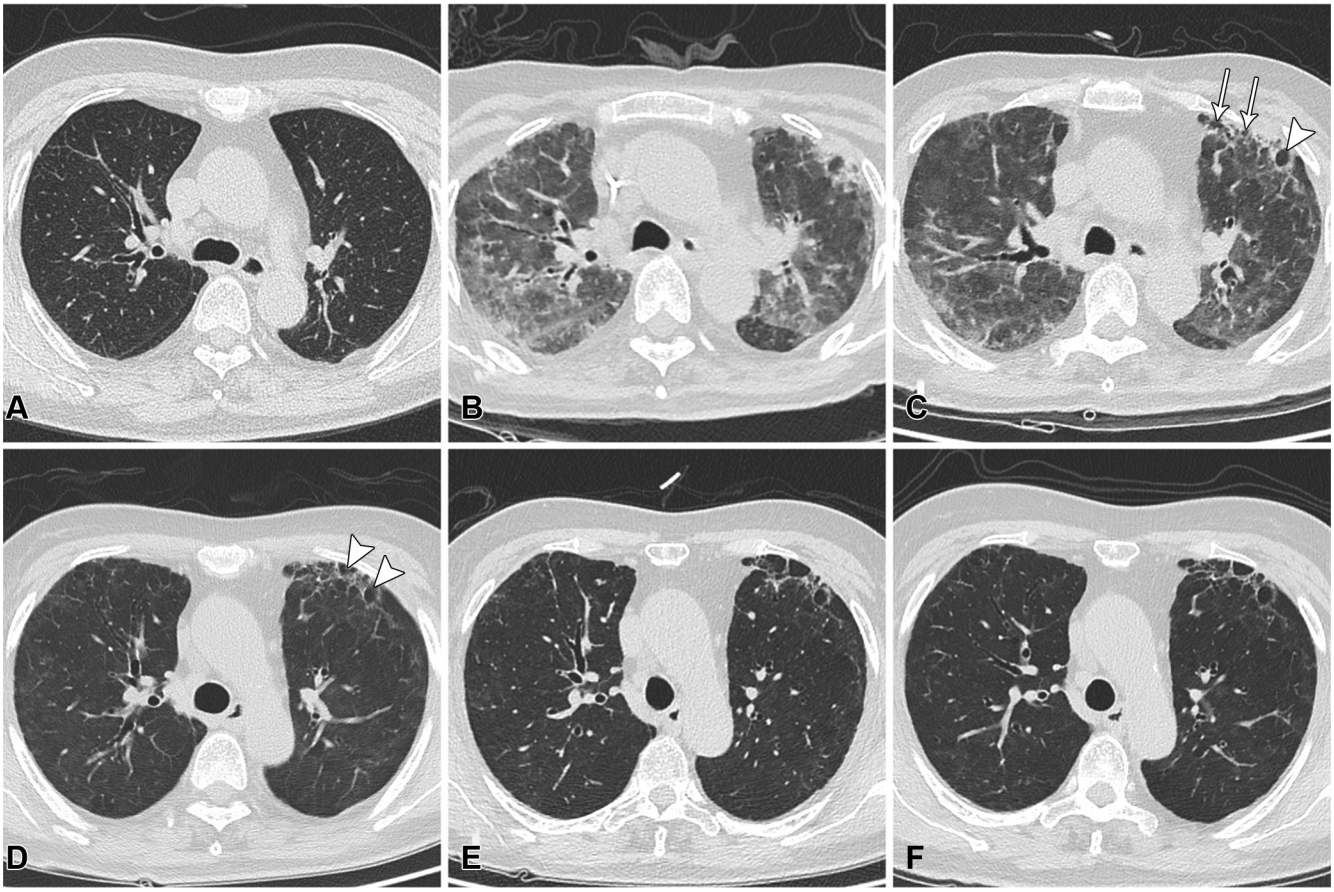

Figure 5: CT scans in 71-year-old man, who progressed to acute respiratory distress syndrome caused by COVID-19, show typical CT findings over time for participants with focally reticular lesions. **(A)** One year before COVID-19, CT scan shows bilateral healthy lungs. **(B)** Twelve days after symptom onset, patient developed aggravated acute respiratory distress syndrome. Emergent CT scan shows diffuse ground-glass opacities (GGOs) with partially subpleural consolidation in bilateral lungs. **(C)** Seventy-six days after symptom onset, CT scan at discharge shows focally subpleural reticular lesions in anterior segment of left upper lobe with cystic airspaces (arrows) and bullae (arrowhead) after partial absorption of GGOs and consolidation. **(D)** Three months after symptom onset, CT scan shows further absorption of GGOs and parenchymal bands, with focally subpleural cystic lesions (arrowheads) remaining in left upper lobe. **(E)** Seven months and **(F)** 12 months after symptom onset, CT scans show slow absorption of bilateral GGOs but stable abnormalities in left upper lobe. All images have same window level of −600 HU and window width of 1600 HU.

ticipants with complete resolution, participants with residual linear opacities or multifocal reticular or cystic lesions demonstrated extensive and diffusive pulmonary involvement at admission (total CT score, 16.0 ± 6.5 vs 7.5 ± 5.8; $P < .001$). Independent risk factors for these residual CT abnormalities at 1 year included age 50 years or older, lymphopenia, and severe or aggravation of acute respiratory distress syndrome.

Similar to previous studies, bilateral subpleural GGOs with partial consolidation and GGOs with parenchymal bands were the most frequent CT findings at admission and discharge, respectively (7–9,11). Any consolidation at admission had been gradually absorbed, typically with a "melting sugar" pattern of resorption whereby the density of consolidation gradually decreases to GGO, but the lesion volume initially enlarges (7,17). After 1 year, complete resolution was observed in 98% of participants with moderate pneumonia (105 of 107) but only in 50% of participants with severe pneumonia or ARDS (51 of 102) ($P < .001$), corroborating the findings of a previous study (7). We found that older age, lymphopenia, and severe or aggravation of ARDS, which correlated with mortality, were risk factors of residual CT abnormalities (4,10,26,27). The presence of multifocal reticular or cystic lesions at discharge was persistent in 28 participants and was accompanied by bronchial dilation in 24 of the 28 participants (86%). Although some articles prompted a potential correlation between mechanical ventilation and these changes, we observed that a high proportion of these participants (12 of 28 [43%]) did not undergo mechanical ventilation therapy (12,17,28,29). Thus, our results suggest that multiple factors contribute to the development of these interstitial lesions and that mechanical ventilation and ARDS are not the only factors.

In a previous study involving 114 participants with severe COVID-19, residual CT abnormalities, including GGO, bronchial dilation, parenchymal bands, and honeycombing, were observed in 62% of recovered participants (71 of 114) after 6 months (17). These CT abnormalities were the typical manifestations of interstitial fibrosis (22,30,31). Our study found a lower rate (25% [53 of 209]) of participants demonstrating CT abnormalities after 1 year (17). Several reasons could explain this difference. First, the previous study included only patients with severe COVID-19, but our participants had COVID-19 of differing severities (17). However, the number of patients

Table 2: Comparison of Characteristics between Two Groups

Characteristic	Participants with Complete Resolution at 12 Months (n = 156)	Participants with Residual CT Abnormalities at 12 Months (n = 53)	P Value
Age (y)*	46 ± 12 (20–82)	60 ± 10 (31–82)	<.001
<50	99 (64)	6 (11)	<.001
≥50	57 (37)	47 (89)	<.001
Sex			
Men	69 (44)	24 (45)	.89
Women	87 (56)	29 (55)	.89
Comorbidity	20 (13)	21 (40)	<.001
COVID-19 severity			
Pneumonia	105 (67)	2 (3.8)	<.001
Severe pneumonia	50 (32)	30 (57)	.001
Acute respiratory distress syndrome	1 (0.6)	21 (40)	<.001
Time from admission to symptom onset (d)*	6.2 ± 4.3 (1.0–17.0)	9.1 ± 4.1 (1.0–18.0)	<.001
≤7	107 (69)	21 (40)	<.001
>7	49 (31)	32 (60)	<.001
Length of hospital stay (d)*	21.0 ± 9.1 (5.0–55.0)	36.1 ± 17.0 (11.0–80.0)	<.001
Laboratory results at admission			
Lymphocyte count ($\times 10^9$/L)*	1.28 ± 0.36 (0.55–3.10)	0.81 ± 0.37 (0.26–1.89)	<.001
<1.10	20 (13)	38 (72)	<.001
≥1.10	136 (87)	15 (28)	<.001
Lactate dehydrogenase level (U/L)*	198 ± 64 (98–480)	352 ± 247 (119–1633)	<.001
≤245	140 (90)	27 (51)	<.001
>245	16 (10)	26 (49)	<.001
Albumin level (g/L)*	35.6 ± 6.0 (22.0–47.7)	30.8 ± 6.6 (20.1–49.6)	<.001
<33	30 (19)	32 (60)	<.001
≥33	126 (81)	21 (40)	<.001

Note.—Except where indicated, data are numbers of participants, with percentages in parentheses. P values comparing participants with complete resolution and participants with residual CT abnormalities were determined using the Mann-Whitney U test or χ^2 test.

* Numbers are means ± standard deviations, with ranges in parentheses.

with severe pneumonia or ARDS was similar between the two studies (83 vs 80 patients and 31 vs 22 patients, respectively) (17). Second, we excluded participants with previous chronic lung disease; their inclusion in the previous study may lead to misjudgments of the lung sequelae not genuinely caused by COVID-19. As a potential indicator of this, predominant reticular lesions (14%), bronchiectasis (11%), and honeycombing (1.8%) at admission were reported previously, which we did not corroborate (17). Our study also found that focally subpleural reticular or cystic lesions and bronchial dilation could be observed at discharge in 30% of the participants (62 of 209) but resolved in more than half of participants within the first 3 months, indicating remodeling of immature fibrosis (12,23). Reversal of these CT abnormalities has also been observed in SARS, other diffuse alveolar damage, and organizing pneumonia (23,32,33). Similar to the findings in SARS, we observed persistent but very focally reticular or cystic lesions only in a small portion of participants with severe COVID-19 and ARDS (15). However, the differentiation of true, irreversible fibrosis from reversible lesions is far from straightforward, and the limited follow-up period in previous studies might result in the overdiagnosis of fibrosis (13,34,35). For these reasons, we avoided radiologic terms such as "traction bronchiectasis," "honeycombing," and "reticular pattern" for their association with genuine lung fibrosis. Instead, we used the terms "bronchial dilation," "subpleural cystic lesions," and "reticular lesions," which were reported to be partially reversible (12,17,22,24).

Our study had limitations. First, there were selection biases. Thousands of discharged participants were excluded because of a lack of chest CT data at admission. The high mortality rate among critically ill participants with COVID-19 had led to the enrollment of only 22 survivors of ARDS (22 of 209 [11%]) (36). Because of the exclusion of participants with previous pulmonary disease, a relatively young cohort (mean age, 49 years) with a low rate of smoking history (1.9%) was reported. Although our approach permitted lung abnormalities to be more definitively attributed to COVID-19, we may have underestimated the long-term effect of COVID-19 on the general population, especially in older patients and patients with a smoking history or previous lung diseases, who probably have more common or more severe lung sequelae (37). Second, it is unknown whether these CT abnormalities will regress after a longer follow-up, thereby meriting further clinical and radiologic follow-up. However, considering that residual lesions rarely change after 1 year in SARS, these CT abnormalities in COVID-19 are likely permanent (15,38). Third, systematic

Table 3: Comparison of CT Findings between Two Groups at Admission and Discharge

Finding	Participants with Complete Resolution at 12 Months (n = 156)	Participants with Residual CT Abnormalities at 12 Months (n = 53)	P Value
Chest CT at admission			
Pulmonary involvement			
Unilateral	31 (20)	3 (5.7)	.02
Bilateral	125 (80)	50 (94)	.02
Pulmonary lesion distribution			
Subpleural	127 (81)	20 (38)	<.001
Diffuse	20 (13)	31 (59)	<.001
Random	9 (5.8)	2 (3.8)	.733
Chest CT abnormality			
Ground-glass opacity	148 (95)	53 (100)	.21
"Crazy paving" pattern	33 (21)	20 (38)	.02
Consolidation	81 (52)	43 (81)	<.001
Predominant CT abnormality			
Ground-glass opacity	97 (62)	23 (43)	.02
"Crazy paving" pattern	14 (9.0)	8 (15)	.21
Consolidation	45 (29)	22 (42)	.09
No. of lobes involved*	3.4 ± 1.6 (1.0–5.0)	4.7 ± 0.9 (1.0–5.0)	<.001
<5	93 (60)	8 (15)	<.001
5	63 (40)	45 (85)	<.001
Total CT score*	7.5 ± 5.8 (1.0–24.0)	16.0 ± 6.5 (2.0–25.0)	<.001
≤10	118 (76)	8 (15)	<.001
>10	38 (24)	45 (85)	<.001
Chest CT at discharge			
Pulmonary involvement			
Unilateral	33 (21)	0 (0.0)	<.001
Bilateral	123 (79)	53 (100)	<.001
Pulmonary lesion distribution			
Subpleural	135 (87)	23 (43)	<.001
Diffuse	14 (9.0)	29 (55)	<.001
Random	7 (4.5)	1 (1.9)	.68
Chest CT abnormality			
Ground-glass opacity	156 (100)	52 (98)	.25
Consolidation	15 (9.6)	22 (42)	<.001
Parenchymal band	99 (64)	53 (100)	<.001
Reticular lesion	21 (14)	41 (77)	<.001
Bronchial dilation	18 (12)	39 (74)	<.001
Volume loss	11 (7.1)	17 (32)	<.001
Subpleural cystic lesion	2 (1.3)	16 (30)	<.001
No. of lobes involved*	3.3 ± 1.5 (1.0–5.0)	4.8 ± 0.6 (2.0–5.0)	<.001
<5	105 (67)	9 (17)	<.001
5	51 (33)	44 (83)	<.001
Total CT score*	5.9 ± 4.4 (1.0–24.0)	14.9 ± 5.6 (3.0–25.0)	<.001
≤10	139 (89)	15 (28)	<.001
>10	17 (11)	38 (72)	<.001

Note.—Except where indicated, data are numbers of participants, with percentages in parentheses. P values comparing participants with complete resolution and participants with residual CT abnormalities were determined using the Mann-Whitney U test, χ^2 test, or Fisher exact test.

* Numbers are means ± standard deviations, with ranges in parentheses.

use of pulmonary function testing was not performed because of use restrictions during the pandemic. This limits our understanding of the functional consequences of CT findings.

In conclusion, 1 year after COVID-19 diagnosis, three chest CT patterns (ie, complete resolution, residual linear opacities, and multifocal reticular or cystic lesions) could be observed, with complete resolution being the most common. Some of the fibrotic lung changes demonstrated at discharge partially resorbed over time, predominantly between discharge and 3 months after symptom onset. Persistent chest CT

abnormalities were more likely to occur in older patients with severe pneumonia, acute respiratory distress syndrome, and lymphopenia. Further studies are needed to determine whether these chest CT findings 1 year after COVID-19 infection are associated with a permanent loss of lung function.

Acknowledgments: We would like to express our sincere gratitude to the emergency services, nurses, doctors, and medical support from other provinces for their efforts to combat the COVID-19 outbreak in Wuhan.

Author contributions: Guarantors of integrity of entire study, F.P., L.Y., C.Z.; study concepts/study design or data acquisition or data analysis/interpretation, all authors;

Table 4: Relationship of Risk Factors with Residual CT Abnormalities after 1 Year

Risk Factor	Univariable Analysis		Multivariable Analysis	
	Odds Ratio*	*P* Value	Odds Ratio*	*P* Value
Age (y) (≥50 vs <50)	13.6 (5.5, 33.8)	<.001	15.9 (4.3, 29.2)	<.001
Comorbidity (yes vs none)	4.5 (2.2, 9.2)	<.001	Excluded	Excluded
COVID-19 severity				
Severe or aggravation of ARDS vs moderate pneumonia	52.5 (7.2, 137.1)	<.001	43.9 (8.1, 239.0)	<.001
Lymphocyte count ($\times 10^9$/L) (<1.10 vs ≥1.10)	17.2 (8.1, 36.8)	<.001	18.9 (6.0, 60.0)	<.001
Lactate dehydrogenase level (U/L) (>245 vs ≤245)	8.4 (4.0, 17.8)	<.001	Excluded	Excluded
Albumin level (g/L) (<33 vs ≥33)	6.4 (3.2, 12.6)	<.001	Excluded	Excluded
No. of lobes involved (5 vs <5)	8.3 (3.7, 18.8)	<.001	Excluded	Excluded
Total CT score (>10 vs ≤10)	17.5 (7.6, 40.3)	<.001	Excluded	Excluded

Note.—ARDS = acute respiratory distress syndrome.
* Numbers in parentheses are 95% CIs.

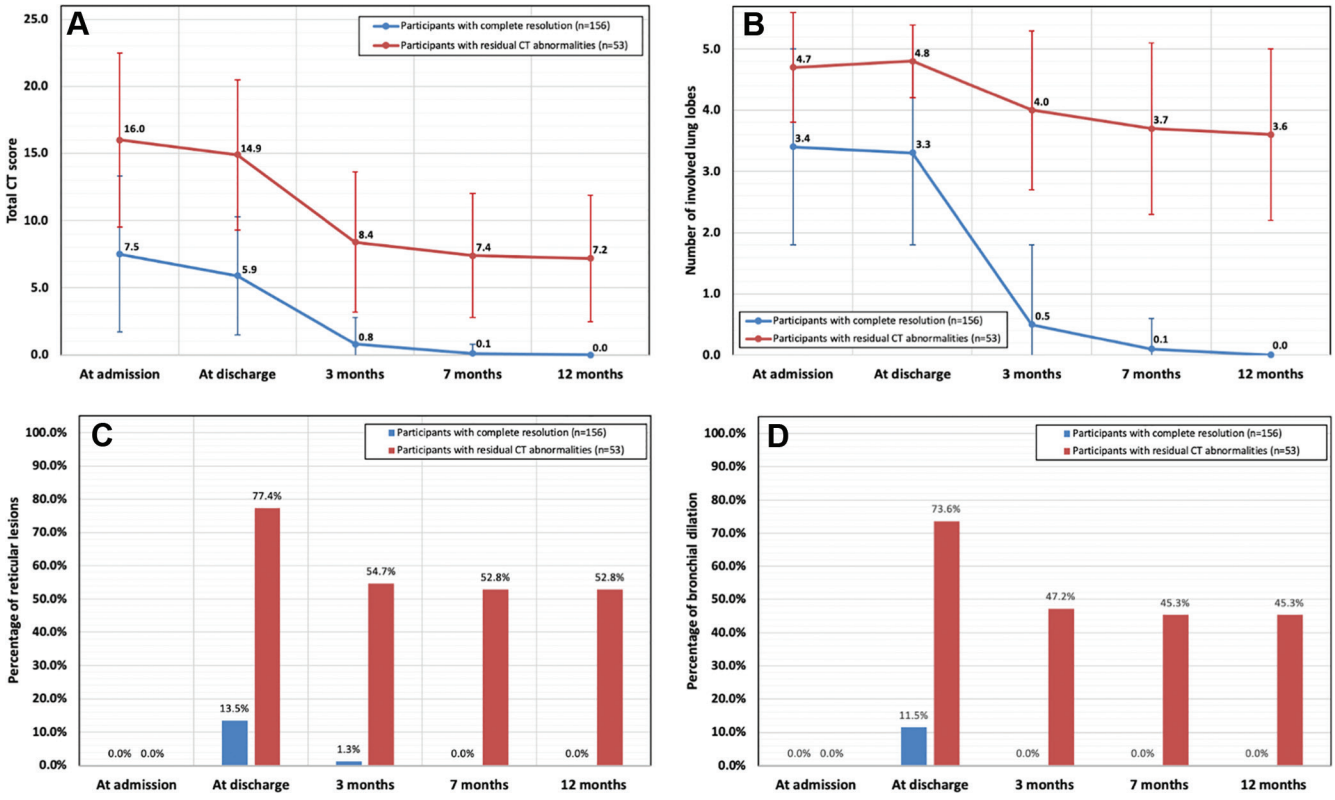

Figure 6: Graphs depict dynamic CT changes over time between participants with complete resolution and residual CT abnormalities at 12 months. Graphs show **(A)** significant differences in total CT score, **(B)** number of involved lung lobes, **(C)** percentages of reticular lesions, and **(D)** percentage of bronchial dilation between the two groups at each time point. Standard deviation bar is shown in **A** and **B**. Linear mixed model of repeated measures was established to estimate fixed effects of time and grouping on total CT score (**A**) and number of involved lung lobes (**B**) using type III tests, and *P* values of multiple comparisons were obtained using Bonferroni adjustments. Significant decreases of mean total CT score (**A**) and number of involved lung lobes (**B**) in both groups were seen at 3 months ($P < .001$ for each comparison). Over time, total CT score (**A**) and number of involved lung lobes (**B**) gradually decreased but were higher in participants with residual CT abnormalities than in participants with complete resolution ($P < .001$ for both comparisons).

manuscript drafting or manuscript revision for important intellectual content, all authors; approval of final version of submitted manuscript, all authors; agrees to ensure any questions related to the work are appropriately resolved, all authors; literature research, F.P., T.Y., Lingli Li, Lin Li, D.L., R.L.H.; clinical studies, F.P., L.Y., B.L., T.Y., Lingli Li, Lin Li, D.L., J.W., C.Z.; statistical analysis, F.P., R.L.H.; and manuscript editing, F.P., L.Y., Lingli Li, Lin Li, D.L., J.W., R.L.H., C.Z.

Disclosures of conflicts of interest: F.P. No relevant relationships. **L.Y.** No relevant relationships. **B.L.** No relevant relationships. **T.Y.** No relevant relationships. **Lingli Li** No relevant relationships. **Lin Li** No relevant relationships. **D.L.** No relevant relationships. **J.W.** Employee of Philips Healthcare. **R.L.H.** No relevant relationships. **C.Z.** No relevant relationships.

References

1. World Health Organization. Weekly epidemiological update on Coronavirus disease (COVID-19) - May 4, 2021. https://www.who.int/docs/default-source/coronaviruse/situation-reports/20210504_weekly_epi_update_38.pdf?sfvrsn=2117260_5&download=true. Published May 4, 2021. Accessed May 5, 2021.
2. Zhou P, Yang XL, Wang XG, et al. A pneumonia outbreak associated with a new coronavirus of probable bat origin. Nature 2020;579(7798):270–273.
3. Yin Y, Wunderink RG. MERS, SARS and other coronaviruses as causes of pneumonia. Respirology 2018;23(2):130–137.
4. Pan F, Yang L, Li Y, et al. Factors associated with death outcome in patients with severe coronavirus disease-19 (COVID-19): a case-control study. Int J Med Sci 2020;17(9):1281–1292.
5. Xu Z, Shi L, Wang Y, et al. Pathological findings of COVID-19 associated with acute respiratory distress syndrome. Lancet Respir Med 2020;8(4):420–422.
6. Meo SA, Alhowikan AM, Al-Khlaiwi T, et al. Novel coronavirus 2019-nCoV: prevalence, biological and clinical characteristics comparison with SARS-CoV and MERS-CoV. Eur Rev Med Pharmacol Sci 2020;24(4):2012–2019.
7. Liu D, Zhang W, Pan F, et al. The pulmonary sequalae in discharged patients with COVID-19: a short-term observational study. Respir Res 2020;21(1):125.
8. Pan F, Ye T, Sun P, et al. Time course of lung changes at chest CT during recovery from coronavirus disease 2019 (COVID-19). Radiology 2020;295(3):715–721.
9. Wang Y, Dong C, Hu Y, et al. Temporal changes of CT findings in 90 patients with COVID-19 pneumonia: a longitudinal study. Radiology 2020;296(2):E55–E64.
10. Pan F, Zheng C, Ye T, et al. Different computed tomography patterns of coronavirus disease 2019 (COVID-19) between survivors and non-survivors. Sci Rep 2020;10(1):11336.
11. Shi H, Han X, Jiang N, et al. Radiological findings from 81 patients with COVID-19 pneumonia in Wuhan, China: a descriptive study. Lancet Infect Dis 2020;20(4):425–434.
12. Wells AU, Devaraj A, Desai SR. Interstitial lung disease after COVID-19 infection: a catalog of uncertainties. Radiology 2021;299(1):E216–E218.
13. Spagnolo P, Balestro E, Aliberti S, et al. Pulmonary fibrosis secondary to COVID-19: a call to arms? Lancet Respir Med 2020;8(8):750–752.
14. Chan KS, Zheng JP, Mok YW, et al. SARS: prognosis, outcome and sequelae. Respirology 2003;8(Suppl 1):S36–S40.
15. Wu X, Dong D, Ma D. Thin-section computed tomography manifestations during convalescence and long-term follow-up of patients with severe acute respiratory syndrome (SARS). Med Sci Monit 2016;22:2793–2799.
16. Li Y, Wu J, Wang S, et al. Progression to fibrosing diffuse alveolar damage in a series of 30 minimally invasive autopsies with COVID-19 pneumonia in Wuhan, China. Histopathology 2021;78(4):542–555.
17. Han X, Fan Y, Alwalid O, et al. Six-month follow-up chest CT findings after severe COVID-19 pneumonia. Radiology 2021;299(1):E177–E186.
18. Balachandar V, Mahalaxmi I, Subramaniam M, et al. Follow-up studies in COVID-19 recovered patients - is it mandatory? Sci Total Environ 2020;729:139021.
19. National Health Commission of the People's Republic of China. Diagnosis and treatment protocols of pneumonia caused by a novel coronavirus (trial version 7). http://www.nhc.gov.cn/yzygj/s7653p/202003/46c9294a7dfe4cef80dc7f5912eb1989/files/ce3e6945832a438eaae415350a8ce964.pdf. Published March 3, 2020. Accessed May 5, 2021.
20. ARDS Definition Task Force; Ranieri VM, Rubenfeld GD, et al. Acute respiratory distress syndrome: the Berlin Definition. JAMA 2012;307(23):2526–2533.
21. World Health Organization. Clinical management of severe acute respiratory infection when novel coronavirus (nCoV) infection is suspected. https://apps.who.int/iris/rest/bitstreams/1272156/retrieve. Published March 13, 2020. Accessed May 5, 2021.
22. Hansell DM, Bankier AA, MacMahon H, McLoud TC, Müller NL, Remy J. Fleischner Society: glossary of terms for thoracic imaging. Radiology 2008;246(3):697–722.
23. Kligerman SJ, Franks TJ, Galvin JR. From the radiologic pathology archives: organization and fibrosis as a response to lung injury in diffuse alveolar damage, organizing pneumonia, and acute fibrinous and organizing pneumonia. RadioGraphics 2013;33(7):1951–1975.
24. Zhang J, Wang S, Shao C. Reversible bronchial dilatation in adults. Clin Exp Pharmacol Physiol 2021;48(7):966–970.
25. Francone M, Iafrate F, Masci GM, et al. Chest CT score in COVID-19 patients: correlation with disease severity and short-term prognosis. Eur Radiol 2020;30(12):6808–6817.
26. Wu C, Chen X, Cai Y, et al. Risk factors associated with acute respiratory distress syndrome and death in patients with coronavirus disease 2019 pneumonia in Wuhan, China. JAMA Intern Med 2020;180(7):934–943.
27. Feng Z, Yu Q, Yao S, et al. Early prediction of disease progression in COVID-19 pneumonia patients with chest CT and clinical characteristics. Nat Commun 2020;11(1):4968.
28. Desai SR, Wells AU, Rubens MB, Evans TW, Hansell DM. Acute respiratory distress syndrome: CT abnormalities at long-term follow-up. Radiology 1999;210(1):29–35.
29. Gupta VK, Alkandari BM, Mohammed W, Tobar AM, Abdelmohsen MA. Ventilator associated lung injury in severe COVID-19 pneumonia patients - case reports: ventilator associated lung injury in COVID-19. Eur J Radiol Open 2020;8:100310.
30. Remy-Jardin M, Giraud F, Remy J, Copin MC, Gosselin B, Duhamel A. Importance of ground-glass attenuation in chronic diffuse infiltrative lung disease: pathologic-CT correlation. Radiology 1993;189(3):693–698.
31. Sverzellati N, Lynch DA, Hansell DM, Johkoh T, King TE Jr, Travis WD. American Thoracic Society-European Respiratory Society classification of the idiopathic interstitial pneumonias: advances in knowledge since 2002. RadioGraphics 2015;35(7):1849–1871.
32. Ooi GC, Khong PL, Müller NL, et al. Severe acute respiratory syndrome: temporal lung changes at thin-section CT in 30 patients. Radiology 2004;230(3):836–844.
33. Xie L, Liu Y, Fan B, et al. Dynamic changes of serum SARS-coronavirus IgG, pulmonary function and radiography in patients recovering from SARS after hospital discharge. Respir Res 2005;6(1):5.
34. Yu M, Liu Y, Xu D, Zhang R, Lan L, Xu H. Prediction of the development of pulmonary fibrosis using serial thin-section CT and clinical features in patients discharged after treatment for COVID-19 pneumonia. Korean J Radiol 2020;21(6):746–755.
35. Huang Y, Tan C, Wu J, et al. Impact of coronavirus disease 2019 on pulmonary function in early convalescence phase. Respir Res 2020;21(1):163.
36. Yang X, Yu Y, Xu J, et al. Clinical course and outcomes of critically ill patients with SARS-CoV-2 pneumonia in Wuhan, China: a single-centered, retrospective, observational study. Lancet Respir Med 2020;8(5):475–481.
37. Çakır Edis E. Chronic pulmonary diseases and COVID-19. Turk Thorac J 2020;21(5):345–349.
38. Zhang P, Li J, Liu H, et al. Long-term bone and lung consequences associated with hospital-acquired severe acute respiratory syndrome: a 15-year follow-up from a prospective cohort study. Bone Res 2020;8(1):8 [Published correction appears in Bone Res 2020;8:34.].